# Advanced systems in medical decision-making using intelligent computing. Application to magnetic resonance imaging

David Jaramillo[1]
1) Department of Computer Architecture and Computer Technology. University of Granada, Spain

Ignacio Rojas[1], Olga Valenzuela[2], Ignacio García[3]
Alberto Prieto[1]
2) Department of Applied Mathematics
3) University Hospital: Virgen de la Nieves.
University of Granada, Spain

*Abstract*— There are several dementias but Alzheimer's Disease (AD) is leading cause of dementia in the world. In this paper, a new methodology for classification of MR images is proposed, using a large data base (more than one thousand patient). We have two main objectives in this paper: a first one where a classification method is developed to classify MR images as either normal or with the Alzheimer's disease and a second which is the ambitious goal of this study, the identification and classification between normal subjects, MCI patients and AD patients. It is noteworthy that with this last study we could offer a tool to assist the early diagnosis of dementia.

**Keywords: Alzheimer's Disease (AD), Mild Cognitive Impairment (MCI), Neuroimaging, Support Vector Machine (SVM), Principal Component Analysis (PCA), Wavelets, Magnetic Resonance Imaging.**

## I. INTRODUCTION

Dementia is an acquired syndrome characterized by a deterioration of higher brain function that determines an impairment of daily life in absence of altered level of consciousness. Still no definitive indicators are known, so the differential diagnosis of dementing illness can be, at least, controversial.

There are several dementias but Alzheimer's Disease (AD) is leading cause of dementia in the world. There are an estimated 35.6 million people in the world with dementia and more than 18 million of them have Alzheimer's disease, which supposes more of the 50% of the total people with dementia. Besides the total number of people with dementia is expected to increase to 65.7 million in 2030 and 115.4 million in 2050.

Today, the diagnosis of Alzheimer's disease is made by using clinical criteria, however these criteria are not able to diagnose the disease in its pre-clinical stage, not offering a early diagnosis. Given this situation, it is necessary to develop methods and techniques to be included in the criteria that provide an early diagnosis, which would allow people with dementia to plan ahead while they still have the capacity to make important decisions about their future care as well as it would allow them to access available drug and non-drug therapies that may improve their cognition and enhance their quality of life.

Neuronal loss and consequent brain atrophy causes widening of the sulci, thinning of the gyri and dilatation of the ventricles with a significant reduction in brain weight. In recent years have been identified different distributions of atrophy depending on the type of dementia. For AD, the atrophy affects the medial temporal lobe (particularly the hippocampus and the entorhinal cortex, posterior cingulated, precuneus, and tempoparietal cortex). However, the measures of the general atrophy do not seem to be useful on the AD diagnosis as most of neurodegenerative diseases cause similar global atrophy.

Many studies have focused on quantifying focal atrophy in the temporal lobe [1] [2] and even exist visual scales to quantify the degree of atrophy, which are quick and easy to use. Recently have been published validations of computerized methods to measure the degree of temporal atrophy. In comparison, these methods have a similar discriminatory power [3] with the advantage that they would facilitate measurements and would provide more objective results by standardizing the methods of analysis [4].

In parallel, there has been observed that AD patients may have a striking atrophy in posterior regions known as posterior cortical atrophy. This impairment seems to be more characteristic, but not exclusive, of AD with typical clinic manifestations and shows in cases of early onset (onset before 65 years). Recently have been proposed visual scales to quantify the degree of posterior cortical atrophy that seems to be useful to discriminate AD from other dementias, especially from frontotemporal dementia (FTD), which also may cause temporal lobe atrophy [5].

From another point of view, computer-based studies look for the acquisition of certain features that lead a classification rule to classify different kind of MR images. In this way, the start point was the classification of MR images of the human brain

as normal or abnormal, thus using wavelets as image features to train a Support Vector Machine (SVM) classifier and using neural network self-organizing maps (SOM), good classification accuracy was achieved [6].

The following studies continued the same line of work as most of them also used wavelets as features and a certain classifier. However, some of them introduced Principal Component Analysis (PCA) as feature reduction algorithm [7] [8]. These last two studies used Neural Networks (NN) for classification. Finally, the final step is to use the developed technique for the classification of specific conditions. So, wavelets and SVM were used to classify mammographic masses from digitalized mammograms as benign or malign [9], and in Alzheimer's disease field, volumetric and shape features together with PCA and SVM were used to classify MR images as having the disease or not [10].

However, most the articles published to date for the use of intelligent classification systems Alzheimer's disease has two major drawbacks:

- They use a low number of data for both training and test (in some cases less than a hundred).
- Classification is performed between patients with dementia and healthy patient, but does not qualify, since it is a complex task, patients with Mild Cognitive Impairment (MCI).

In this paper, a new methodology for classification of MR images is proposed using a large data base (more than one thousand patient), for the classification of MCI patients. We have two main objectives in this paper: a first one where a classification method is developed to classify MR images as either normal or with the Alzheimer's disease and a second which is the ambitious goal of this study, the identification and classification between normal subjects, MCI patients and AD patients. It is noteworthy that with this last study we could offer a tool to assist the early diagnosis of dementia. Besides, throughout the entire paper different techniques and methods are tested to compare them and determine which are those that offer better results.

## II. ALZHEIMER'S DISEASE ON MAGNETIC RESONANCE IMAGING

Imaging findings in patients with MCI are typically inconspicuous, and often considered as normal. The main problem is that do not exist standardized criteria to determine if the impairment observed in a MR image is caused by normal aging or if it can be admitted as pathological. After 65 years is considered normal to detect mild signs of atrophy and little impairments of the white matter, but the evaluation of the degree of damage, which will determine if it is considered pathological, remains subjective [11].

The table below shows the principal slices were AD symptoms could be detected. The main feature of the disease is the general atrophy of the cerebral cortex. As the disease progresses, an accelerated loss of focal volume is shown in the medial temporal lobes, in particular in the hippocampus, entorhinal cortex and amygdala.

| Healthy Patient | Patient with AD | Observations |
|---|---|---|
| 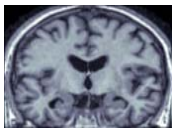 | 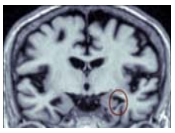 | In clinical practice, the width of the horn of the lateral ventricle is the most reproducible measure to asses the atrophy. |
| 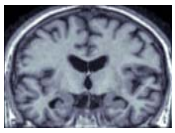 | 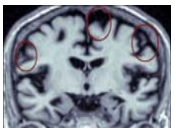 | Cortical volume loss. General atrophy of the cortex. |
| 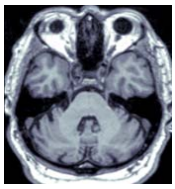 | 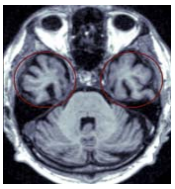 | Atrophy of the temporal lobes. |
| 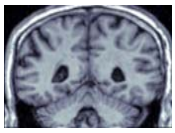 | 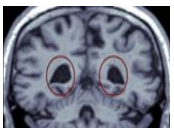 | Dilatation of the ventricular system as a result of general atrophy. |
| 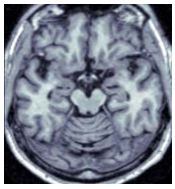 | 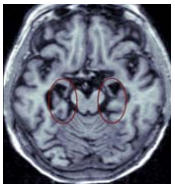 | Atrophy in the hippocampal region. |
| 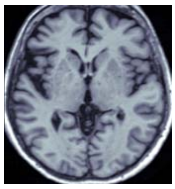 | 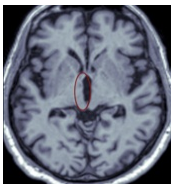 | It is possible to observe the dilatation of the third ventricle. |

*Table 1. Alzheimer's disease on MRI*

## III. MATERIALS AND METHODS

ADNI (Alzheimer's Disease Neuroimaging Initiative) beginning in 2004 is a 7-year massive effort to support research in the discovery and development of treatments that slow or stop the progression of AD. ADNI is a multisite longitudinal clinical/imaging/genetic/biospecimen/biomarker study. Its goal is to determine the characteristics of AD as the pathology that evolves from normal aging to mild symptoms, to MCI, to dementia. ADNI is committed to establishing standardized methods for imaging/biomarker collection and analysis for use in clinical trials.

In the Figure 1 are shown the eight cores that structure ADNI. In this paper we are only interested in the MRI core, based at

the Mayo Clinic, Rochester, Minnesota, and responsible for all MRI procedures and for developing standardized imaging methods.

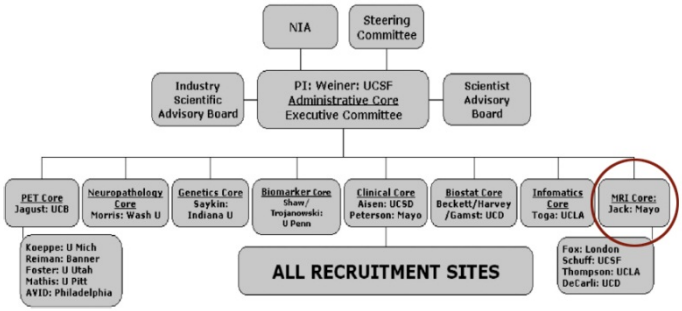


*Figure 1. Governance and organization of ADNI*

Describing the past, present and the future of the ADNI MRI core, it starts with the "ADNI-1" for the first 5 years (approximately, from 2005 to 2010). Focusing on the MR images, all subjects enrolled in this period received a 1.5T protocol examination at multiple point times which varied by baseline clinical diagnosis: MCI at 0, 6, 12, 24 and 36 months; AD at 0, 6, 12 and 24 months; and controls at 0, 6, 12, 24 and 36 months. A subset of participants (approximately 25%) was enrolled in a 3T arm, which involved MRI scanning at both 1.5T and 3T at each scheduled time. ADNI-1 ended October 2010.

Plans for the second 5 years of ADNI running through 2015 are based on "ADNI-GO" (GO stands for "Grand Opportunity") and "ADNI-2", which is the 5-year competitive renewal of ADNI-1. These initiatives are following three cohorts of subjects:

- Cognitively normal and late MCI subjects carried forward from ADNI-1 (followed at 1.5T).
- Early MCI enrolled in ADNI-GO and carried forward into ADNI-2 (scanned at 3T).
- Cognitively normal, late MCI and AD subjects newly enrolled in ADNI-2 (scanned at 3T).

Thus, the initiatives described above provide us a great database of MR images that are used in this paper. Specifically, for the realization of this study were downloaded 1500 images with a total size of approximately 240 GB. Once they were normalized and some images with errors were eliminated, 1350 images (443 are from cognitively normal subjects, 448 from MCI subjects and 459 from AD subjects) are left with a size of 15.7 MB each one, which makes a database of normalized MR images with a size of approximately 21 GB. The extension of the files is .nii, which corresponds to the format NIfTI (Neuroimaging Informatics Technology Initiative). This format is adapted from the widely used ANALYZE 7.5 using the "empty space" in its header to add new features. For more information see the official website of ADNI [12].

In studies that involve images of many patients, it is often useful (in this paper necessary) to coregister a brain image of a patient to that of another subject or a standard template. We refer to this process as spatial normalization.

To perform the normalization of our MR images we used the "SPM5" (currently available SPM8 release) toolbox for MATLAB. SPM (Statistical Parametric Mapping) entails the construction of spatially extended statistical processes to the test hypotheses about regionally specific effects [13]

## IV. FEATURE EXTRACTION

In this paper, we need to extract from an image the feature vector that characterizes it. Thus, our features are the approximate wavelet coefficients, using them to generate a classification rule to assist with diagnosis. As described in the following sections the number of features is not as important as robustness to get the best classification accuracy, being robustness in an image application understood as the consistency of the results that certain feature provides across the entire application.

Wavelets are mathematical functions that decompose data into different frequency components and then study each component with a resolution matched to its scale. While the Fourier Transform only provides representation of an image based on its frequency content, so it loses time information of the signal, the Wavelet Transform provides both time and frequency information (see Figure 2). Therefore, the Wavelet Transform is a better tool for feature extraction from images.

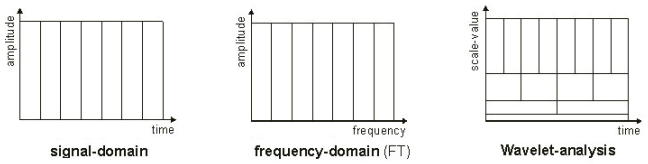


*Figure 2. The development of signal analysis*

The Discrete Wavelet Transform (DWT) is a linear transformation that operates on a data vector whose length is an integer power of two, transforming it into a numerically different frequency components, and then studies each component with resolution matched to its scale.

Supposed *x(t)* a square - integrable function, then the continuous wavelet transform of *x(t)* relative to a given wavelet ψ(t) is defined as:

$$(1)\ W_{\Psi}(a,b) = \int_{-\infty}^{\infty} x(t)\psi_{a,b}(t)dt$$

where

$$(2)\ \psi_{a,b}(t) = \frac{1}{\sqrt{a}}\psi\left(\frac{t-a}{b}\right)$$

To get the DWT, equation 1 can be discretized by restraining a and b to a discrete lattice (a = 2b; a > 0; a, b ∈ ℜ). Then, the DWT can be expressed as follows:

$$ca_{j,k}(n) = DS\left[\sum_n x(n) g_j^*(n - 2^j k)\right]$$

$$cd_{j,k}(n) = DS\left[\sum_n x(n) h_j^*(n - 2^j k)\right]$$

Here $ca_{j,k}$ and $cd_{j,k}$ refer to the coefficients of the approximation components and detail components, respectively. *g(n)* and *h(n)* denote the low-pass filter and high-pass filter, respectively. *j* and *k* represent the wavelet scale and translation factors, respectively; and *DS* operator means the down sampling [14].

The above decomposition process can be iterated decomposing successively the approximations in turn, so that the signal is broken down into various levels of resolution. In case of images, the DWT is applied to each dimension separately, decomposing an image into four sub-bands which are low-low (LL), low-high (LH), high-high (HH) and high-low (HL); where the LL sub-band can be regarded as the approximation component and it is used for the next level of the 2D-DWT, meanwhile the other sub-bands would be regarded as the detailed component of the image. A 2D-DWT scheme is shown in Figure 3.

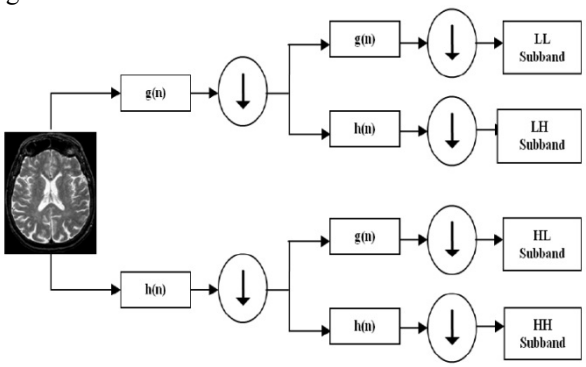


*Figure 3. 2D DWT decomposition scheme*

Figure 4 shows the decomposition up to level 2 of an image using the Wavelet Toolbox of MATLAB and Figure 23 shows how the approximation and detailed components are organized.

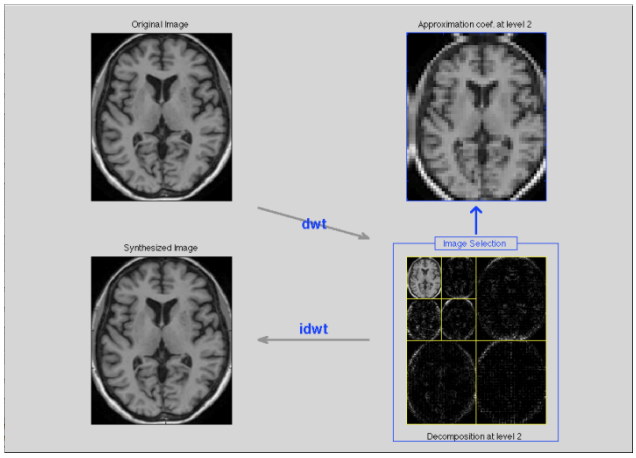


*Figure 4. Level 2 decomposition of an image using DWT*

At each decomposition level, the half band filters produce signals spanning only half the frequency bands. This makes the frequency resolution two when the indetermination in frequency becomes a half less [9], the size of the first level approximation coefficients of an N by N image is N/2 by N/2, the second level is N/4 by N/4 and so on. As the level decomposition is increased, a more compact and less resolution image is obtained [6].

## V. FEATURE SELECTION

Often the extraction of image features provides a large number of them, but as we explained before, that do not guarantee the best classification accuracy because of a part of the data may be redundant. Therefore, we have used the Principal Component Analysis (PCA) in our experiments as a feature reduction technique and also have studied the effects of including other two techniques that set a ranking of features in order of importance based on different criteria: minimum Redundancy Maximum Relevance (mRMR) and Normalized Mutual Information Feature Selection (NMIFS).

## VI. CLASSIFICATION

For the classification of the MR images we used Support Vector Machines technique. In particular, the LIBSVM 3.0.1 (currently available the 3.1.1 version), which is an integrated software for SVM classification with a MATLAB extension [15]. The best enhancement that LIBSVM provides is the multi-class classification, while most of SVM tools only can classify between two classes

Firstly, we defined the procedure to follow. In the first place, we use the 2D-DWT to perform the feature extraction, then we develop a feature selection algorithm based on PCA and finally we use an SVM classifier. The structure of the procedure is schematically shown at Figure 5.

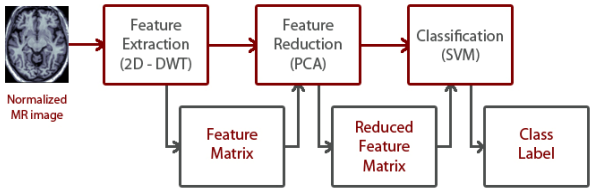


*Figure 5. Structure of Experiment I schematically*

Once the procedure was decided, we had to know what slice or slices where the best to extract the wavelets from them. According to this, we proposed two starting points: a first in which we have no medical expert help and a second in which Doctor Ignacio García Basterra (Neurologist) advises us the slices where the AD can be diagnosed. Thus, in the first option, we have applied the complete procedure shown in Figure 5 to every slice of every image to set up a ranking of accuracy. Then we used the top 20 slices in the experiment.

The first interesting result is to verify the difference between the slices chosen by the computer and the expert. According to this, in the coronal view the slices are quite similar, so the same brain zones are included in the studies. However, while Dr

García chose those slices where the temporal lobes can be clearly observed together with the hippocampus, our procedure gives us higher slices where only the hippocampus can be observed.

| No. of Classes | Medical Expert | Wavelet Family | No. of Patients | No. of Features | No of. PC. | Final Feat. Matrix |
|---|---|---|---|---|---|---|
| 2 (NAD) | No | Db4 L2 | 902 | 40144 | 369 | 902x369 |
| 2 (NAD) | Yes | Db4 L2 | 902 | 40144 | 408 | 902x408 |
| 2 (NAD) | No | Haar L3 | 902 | 8400 | 297 | 902x297 |
| 3 (NMCIAD) | No | Db4 L2 | 1350 | 56784 | 597 | 1350x597 |
| 3 (NMCIAD) | No | Haar L3 | 1350 | 12000 | 466 | 1350x466 |

*Table 2. Matrices of features after Feature Extraction process*

## VII. Classification Accuracy

This is the final step of the procedure. Based on the studies cited earlier, we find that two wavelet families are mainly used: the Daubechies - 4 wavelet up to level 2 and the Haar wavelet up to level 3. We decided to study both and see which one gives better results.

Therefore at this point, we have five matrices of features, each one according to a different study. Then, we use PCA to reduce the dimensions of features to a higher degree. Once we have the principal components and their associated variances, we keep a number of them that preserves 95% of total variance. Hence, the number of principal components kept is the number of features for each patient that conforms the final feature matrix. To clarify, the development of the five studies can be followed in the Table 2 where is shown the final number of features for each subject after the feature reduction is applied.

From now on we noted as NAD those experiments that involves two classes classification (normal and AD images), and as NMCIAD those that involves the three different kind of subjects (normal, AD and MCI).

| Study | Accuracy (%) |
|---|---|
| Db4 L2 + RBF Kernel | 98.7 |
| Db4 L2 + RBF Kernel (Medical Expert) | 97.3 |
| Haar L3 + RBF Kernel | 98.7 |
| Db4 L2 + Linear Kernel | 94.7 |

*Table 3. Accuracy of the NAD studies*

We implement the SVM classifier with LIBSVM. So, we use the RBF kernel as the main kernel of the experiment, however, we also use the linear kernel to study the variance of the results against the RBF kernel. Once we have decided to use the RBF kernel, the goal is to identify good (C, γ) so that the classifier can accurately predict unknown data (i.e. testing data). A common strategy is to use Cross - Validation (CV) that is to separate the data into two parts, of which one is considered unknown. The prediction accuracy obtained from "unknown" set more precisely reflects the performance on classifying an independent data set. In p - fold CV, we first divide the training set into p subsets of equal size. Sequentially one subset is tested using the classifier trained on the remaining $p - 1$ subsets. Thus, each instance of the whole training set is predicted once so the CV accuracy is the percentage of data which are correctly classified. Finally, we chose to do a "grid - search" on C and ɣ using p - fold CV. Various pairs of (C, γ) values are tried and the one with the best CV accuracy is picked.

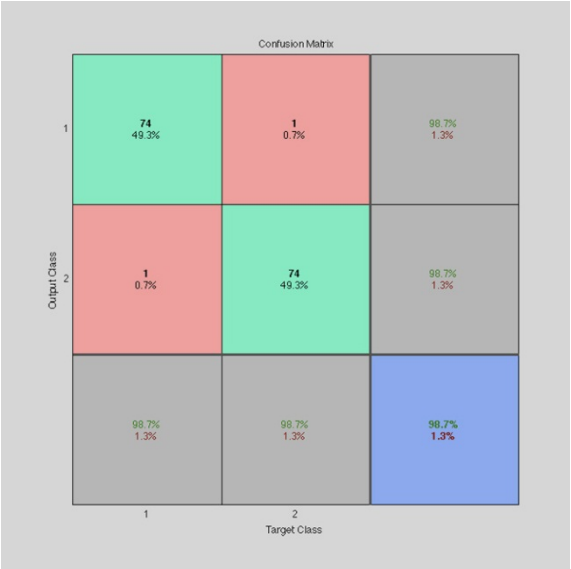


*Figure 6. Confusion Matrix. Study: NAD+Db4L2+RBF*

We chose to use 75 MR images of each class for testing making a total of 150 images (the 16.63% of the whole database, i.e. 902 images) for testing in two classes classification (NAD) and 225 (the 16.67% of the whole database, i.e. 1350 images) in three classes (NMCIAD). It is noteworthy that the images used for testing are not included in the training set.

Tables 3 and 4 show the accuracy achieved by the seven studies performed for NAD and NMCIAD classification respectively.

We have obtained very good accuracy results with the four studies of NAD classification. According to them, is quite difficult to choose between the wavelet families used as both have the same accuracy. However, because the haar family provides fewer features, the computational time is lower, so it might be a better option. In what refers to the kernel choice, although the linear kernel achieves a really good accuracy, the

probability estimates for each class label are clearly lower than the same with the RBF kernel.

| Study | Accuracy (%) |
|---|---|
| Db4 Level 2 + RBF Kernel | 90.2 |
| Haar Level 3 + RBF Kernel | 86.2 |
| Db4 Level 2 + Linear Kernel | 89.8 |

*Table 4. Accuracy of the NMCIAD studies*

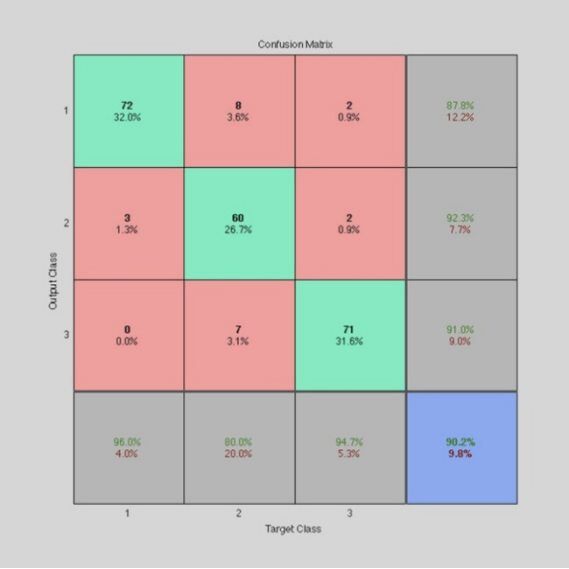


*Figure 7. Confusion Matrix. Study: NMCIAD+Db4L2+RBF*

Finally, Figures 6 and 7 show the confusion matrix for the two studies of each class (NAD and NMCIAD) which have achieved the best classification accuracy.

On the other hand, as it is mentioned on this text before, we have implement two feature selection methods based on mRMR and NMIFS rankings respectively. Once the rankings are set, we have repeated the whole procedure of the Experiment I for the main studies to obtain the classification accuracy using the first 10, 20, 30, 50, 100 and 200 features for the NAD classification and the first 10, 20, 30, 50, 100, 300 and 450 features for the NMCIAD classification problem.

The results achieved using both feature selection methods are shown on Table 5.

## VIII. Sensitivity, Specificity and Predictive Values

Sensitivity, specificity and predictive values are statistical measures of the performance of a diagnostic method. Each subject in this paper either has or does not have the disease. The test outcome can be positive (predicting that the person has the disease) or negative (predicting that the person does not have the disease). The test results for each subject may or may not match the actual status of the subject. In that setting:

- TP (True Positive): Sick people that is correctly diagnosed as sick.
- FP (False Positive): Healthy people that is incorrectly identified as sick.
- TN (True Negative): Healthy people that is correctly identified as healthy.
- FN (False Negative): Sick people that is incorrectly identified as healthy.

| | No. of Selected Features | mRMR Accuracy (%) | NMIFS Accuracy (%) |
|---|---|---|---|
| NAD | 10 | 70.7 | 62.0 |
| | 20 | 80.0 | 84.7 |
| | 30 | 86.7 | 89.3 |
| | 50 | 93.3 | 88.7 |
| | 100 | 97.3 | 94.7 |
| | 200 | 97.3 | 98.0 |
| | 369 | 98.7 | 98.7 |
| NMCIAD | 10 | 62.7 | 60.0 |
| | 20 | 77.8 | 73.4 |
| | 30 | 65.8 | 73.4 |
| | 50 | 76.0 | 79.2 |
| | 100 | 82.7 | 89.4 |
| | 300 | 86.2 | 85.4 |
| | 450 | 87.1 | 87.6 |
| | 597 | 90.2 | 90.2 |

*Table 5. Classification accuracy with Feature Selection using mRMR and NMIFS*

Sensitivity measures the proportion of actual positives which are correctly identified as such, i.e. the percentage of sick people who are correctly identified as having the condition. This can also be written as:

$$Sensitivity = \frac{TP}{TP + FN}$$

Specificity measures the proportion of negatives which are correctly identified, i.e. the percentage of healthy people who are correctly identified as not having the condition. This can also be written as:

$$Specificity = \frac{TN}{TN + FP}$$

The Positive Predictive Value (PPV) is the proportion of subjects with positive test results who are correctly diagnosed. It reflects the probability that a positive test reflects the underlying condition being tested for. It is defined as:

$$PPV = \frac{TP}{TP + FP}$$

The Negative Predicted Value (NPV) is defined as the proportion of subjects with a negative test result who are correctly diagnosed. It is very important to have a high NPV as it means that the test only rarely misclassifies a sick person as being healthy. It is defined as:

$$NPV = \frac{TN}{TN + FN}$$

Tables 6 and 7 show the sensitivity, specificity, PPV and NPV achieved in our studies for NAD and NMCIAD classification respectively.

| Study | Sensitivity | Specificity | PPV | NPV |
|---|---|---|---|---|
| Db4 L2 + RBF Kernel | 0.987 | 0.987 | 0.987 | 0.987 |
| Db4 L2 + RBF Kernel (M. E.) | 0.960 | 0.987 | 0.986 | 0.961 |
| Haar L3 + RBF Kernel | 0.987 | 0.987 | 0.987 | 0.987 |
| Db4 L2 + Linear Kernel | 0.933 | 0.960 | 0.959 | 0.935 |

*Table 6. Sensitivity, specificity, PPV and NPV of the NAD studies*

It is noteworthy that as these measures belong to binary classification tests, in the case of three classes we have to adapt them. Thus, we show the sensitivity and PPV referred to a certain disease (MCI or AD).

| Study | Sensitivity (MCI) | Sensitivity (AD) | Specificity | PPV (MCI) | PPV (AD) | NPV |
|---|---|---|---|---|---|---|
| Db4 L2 + RBF Kernel | 0.800 | 0.947 | 0.960 | 0.923 | 0.910 | 0.878 |
| Haar L3 + RBF Kernel | 0.693 | 0.947 | 0.947 | 0.881 | 0.877 | 0.835 |
| Db4 L2 + Linear Kernel | 0.787 | 0.947 | 0.960 | 0.922 | 0.922 | 0.857 |

*Table 7. Sensitivity, specificity, PPV and NPV of the NMCIAD studies*

## IX. CONCLUSION

In this paper an important challenge has been analyzed: the necessity of identifying the condition prior to dementia which is Mild Cognitive Impairment (MCI) and the development of an intelligent classifier, which using the information of magnetic resonance imaging, can successfully classifies different patients according to their condition. Subjects with MCI are in an intermediate clinical situation between normality and dementia, which is characterized by the presence of subjective cognitive complaints but that do not make a significant alteration in activities of daily living. As there are studies that show that between the 10 and 15% of patients with MCI have developed dementia within a year, it is really important to be able of identify this pathology. Thus, it is in this field where imaging techniques can play a key role in early detection of patients who can develop dementia, in differential diagnose of distinct dementias and monitoring the disease progression differential diagnose of distinct dementias and monitoring the disease progression. According to this and considering that a medical test that presents sensitivity or specificity over 80% is considered as good, together with the classification accuracy shown we have achieved great results.

In this paper, Discrete Wavelet Transform (DWT) has been used for feature extraction, Principal Component Analysis (PCA) for feature reduction, and different methodologies, such as minimum Redundancy Maximum Relevance (mRMR) and Normalized Mutual Information, as feature selection. Finally, the SVM has been used for classification, obtaining excellent results.

About the two feature selection algorithms tested (mRMR and NMIFS), it does not worth to use them, as the computational time needed to set up the ranking is clearly higher than the computational time to run the process with all the features. Specifically in NMCIAD classification this time is prohibitive. Another future work would be to use these algorithms instead of PCA and to study how affects the results.

## ACKNOWLEDGMENT

This paper has been partially supported by the Spanish CICYT Project SAF2010-20558 and Regional Excellent Project P07-TIC-02768 and P09-TIC-175476.

## REFERENCES

[1] Scheltens, P., Frisoni, G. B., Galluzzi, S., Nobili, F. M., Fox, N. C., Robert, P. H., et al. (2003). Neuroimaging tools to rate regional atrophy, subcortical cerebrovascular disease, and regional cerebral blood flow and metabolism: consensus paper of the EADC. Neurol Neurosurg Psychiatry , 71, 1371-81.

[2] Koedan, E., Lehmann, M., Van der Flier, W. M., Scheltens, P., Pijnenburg, Y., Fox, N., et al. (2011). Visual assessment of posterior atrophy development of a MRI rating scale. Eur Radiol , 21, 2618-2615.

[3] Westman, E., Cavallin, L., Muehlboeck, J. S., Zhang, Y., Mecocci, P., Vellas, B., et al. (2011). Sensitivity and Specificity of Medial Temporal Lobe Visual Ratings and Multivariate Regional MRI Classification in Alzheimer's Disease. *PLoS One , 6* (7).

[4] Jack, C. R., Barkhof, F., Barnstein, M. A., Cantillon, M., Cole, P. E., DeCarli, C., et al. (2011). Steps to standardization and validation of hippocampal volumetry as a biomarker in clinical trials and diagnostic creiterion for Alzheimer's disease. *Alzheimer's & Dementia , 7*, 474-485.

[5] Koedan, E., Lehmann, M., Van der Flier, W. M., Scheltens, P., Pijnenburg, Y., Fox, N., et al. (2011). Visual assessment of posterior atrophy development of a MRI rating scale. *Eur Radiol , 21*, 2618-2615.

[6] Chaplot, S., Patnaik, L., & Jagannathan, N. R. (2006). Classification of magnetic resonance brain images using wavelets as input to support vector machine and neural network. *Biomedical Signal Processing and Control , 1*, 86-92.

[7] El-Dahshan, E. A., Salem, A. M., & Younis, T. H. (2009). A hybrid technique for automatic MRI brain images classification. *Studia Univ. Babes-Bolyai, Informatica , 54* (1).

[8] Zhang, Y., Zhengchao, D., Wu, L., & Wang, S. (2011). A hybrid method for brain image classification. *Expert Systems with Applications , 38*, 10049-53

[9] Gorgel, P., Sertbas, A., Kilic, N., Ucan, O., & Osman, O. (2009). Mammographic mass classification using wavelet based suppont vector machine. *Journal of Electrical & Electronics Engineering , 9* (1), 867-875.

[10] Lee, J., Su, S., Huang, C., Wang, J. J., Xu, W., Wei, Y., et al. (2009). Combination of multiple features in support vector machine with

principal component analsis in application for Alzheimer's disease diagnosis. *Lecture Notes in Computer Science , 5863*, 512-519.

[11] Pérez, D. A., Ramos, A., & Álvarez-Linera, J. (2010). *Neuroimagen. Diagnóstico, técnicas, secuencias 2*. Almirall.

[12] LONI. (2011). Retrieved November 5, 2011, from ADNI (Alzheimer's Disease Neuroimaging Initiative): adni.loni.ucla.edu

[13] Friston, K. J., Frith, C. D., Liddle, P. F., & Frackowiak, R. (1991). Comparing functional (PET) images: the assessment of significant change. *J. Cereb. Blood Flow Metab. , 11*, 690-699.

[14] Nanni, L., & Lumini, A. (2008). Wavelet decomposition tree selection for palm and face authentication. *Pattern Recognition Letters , 29* (3), 343-353

[15] Chan, C., & Lin, C. (2011). LIBSVM: a library for support vector machines. *ACM Transactions on Intelligen Systems and Technology , 2* (3), 2:27:1-27:27.